Audio Engineering Society
Convention Paper
Presented at the 117th Convention
2004 October 28–31 San Francisco, CA, USA

Jump Resonance in Audio Transducers

Ali Jabbari[1], and Andrew Unruh[1]

[1] Tymphany Corporation, Cupertino, CA, 95014, US
ali@tymphany.com
andy.unruh@tymphany.com

ABSTRACT

The resonance behavior of a driver with low damping is studied. In such a system, the existing nonlinearities can result in jump resonance, a bifurcation phenomenon with two regimes. One regime, accompanied by a sudden decrease in amplitude, is evident when the frequency of excitation is increasing. The other regime, exhibiting a sudden increase in amplitude, is present when the frequency of excitation is decreasing. Jump resonance was experimentally observed in an audio transducer with low damping and subsequently confirmed by analysis and simulation using a detailed dynamic model that includes the most significant sources of nonlinearities. The conclusion of this work is that the primary cause of jump resonance in audio transducers is the nonlinearity in the driver compliance. The importance of this phenomenon increases as the use of current amplifiers becomes more widespread, since the resulting low system damping makes jump resonance more likely.

1. INTRODUCTION

Mechanical systems with energy storing elements, such as a mass-spring system, exhibit the familiar resonance behavior. In such a system, under low damping conditions, at resonance, the system will vibrate at a high amplitude, with minimal excitation. That is, at the resonance frequency, the system gain from the excitation input to the amplitude of vibration is very high. It is well known that the magnitude of this gain depends on the extent of the damping that is present in the system (e.g. friction, viscous damping, BEMF). Furthermore, the resonance frequency depends on the ratio of the equivalent stiffness and mass of the system. For example, higher stiffness results in a higher resonance frequency, and higher mass results in a lower resonance frequency.

In an ideal linear system, the resonant behavior is well understood. In such systems, the maximum gain from the excitation amplitude to the amplitude of oscillation occurs at a specific frequency. Additionally, for a given amplitude of excitation, the amplitude of oscillation changes smoothly as excitation frequency is increased or decreased. However, when nonlinear elements are present in the system, such as nonlinear restoring forces, the resonant behavior of the system undergoes a qualitative change. This is particularly true when the system damping is low, resulting in large amplitudes of oscillation as resonance frequency is approached. When such a system is swept with a chirp signal, the peak amplitude of oscillation and the frequency at which it

occurs depend on the direction – increasing or decreasing frequency – of the chirp signal.

A typical electromagnetic driver, used in most audio transducers, behaves much like a mass-spring system. This is particularly true at frequencies well below the cone breakup frequencies. There are however many nonlinear elements in such drivers. The most significant of those are the nonlinearities in the restoring force, the BL factor, and the inductance. Given that these nonlinearities are functions of driver cone displacement, the transducer behaves linearly for small excursions. As the cone excursion increases, the effects of nonlinearities become more prominent, resulting in harmonic and intermodulation distortion. Furthermore, when the driver damping is low, these nonlinearities significantly change the resonant behavior of the driver.

The motivation for the analysis, presented in this paper, is the experimental observation of sudden jumps in the amplitude of driver excursion near its resonance frequency. This is manifested as either a sudden decrease or a sudden increase in the amplitude of oscillation, depending on the direction from which the resonance frequency is approached. When the resonance frequency is approached from a higher frequency there is a sudden increase in the amplitude of oscillation. On the other hand, when the resonance frequency is approached from a lower frequency, there is a sudden decrease in the amplitude of oscillation. Furthermore, the frequencies at which these jumps in the amplitude of cone excursion occur are distinct, which is representative of a bifurcation phenomenon. In a typical driver, due to the stiffening nature of the restoring force, the jump to higher amplitude of oscillation occurs at a lower frequency than the frequency at which the jump to lower amplitude of oscillation occurs.

A detailed dynamic model of a typical audio transducer is developed in order to investigate the observed jump resonance behavior. The model includes the more significant nonlinearities present in a typical driver, namely the nonlinearities in the BL factor, inductance, and compliance. The resulting dynamic model is used to determine which of the aforementioned nonlinearities significantly contribute to the onset of the jump resonance behavior. Furthermore, with this model, the effect of varying these nonlinearities and the resulting effect on the jump phenomenon can be studied.

An analytical treatment of the jump resonance phenomenon is given for both the undamped and damped forced oscillation. The effect of softening and hardening spring, as well as that of increasing system damping is presented.

2. NONLINEAR MODEL OF A DRIVER

To investigate the effects of various nonlinearities on the behavior of a typical driver, a nonlinear model of such a driver was created. The model is implemented in Matlab and its graphical interface, Simulink [5,6]. There are two main components in the model, namely, the mechanical and the electrical subsystems. Each subsystem includes the appropriate nonlinear elements and the governing differential equations. In each subsystem the various internal states of the system, and significant parameters and quantities such as forces, voltages, inductance, BL-factor and others can be monitored. The two subsystems are interconnected to each other, as shown in Figure 1.

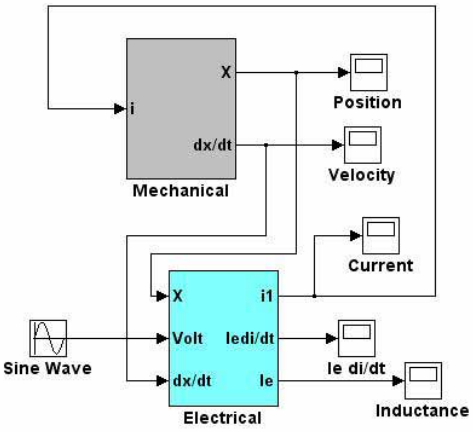

Figure 1: Mechanical and Electrical Subsystems

The mechanical subsystem models the driver as a point mass, with a single degree of freedom in x, attached to a nonlinear spring, and a linear mechanical damper. The electromagnetic force applied to the point mass is determined by the current output of the electric block and the value of the nonlinear BL factor, see equation 1.

$$F = BL(x) \cdot i \qquad (1)$$

It is assumed that the BL factor can be represented as a nonlinear function of the position of the point mass.

$$BL(x) = \sum_{i=0}^{n} b_i x^i \qquad (2)$$

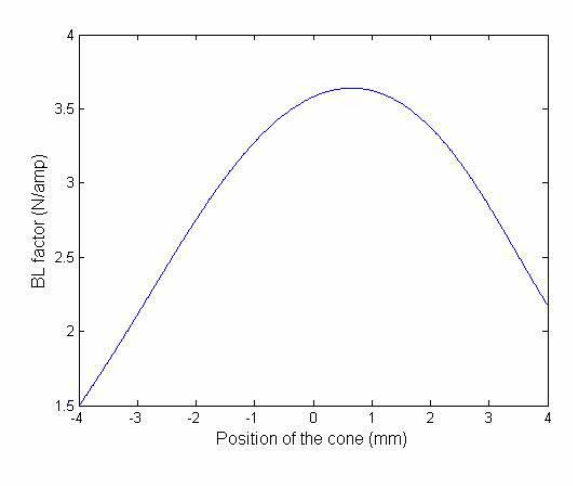

Figure 2: BL curve for a typical driver

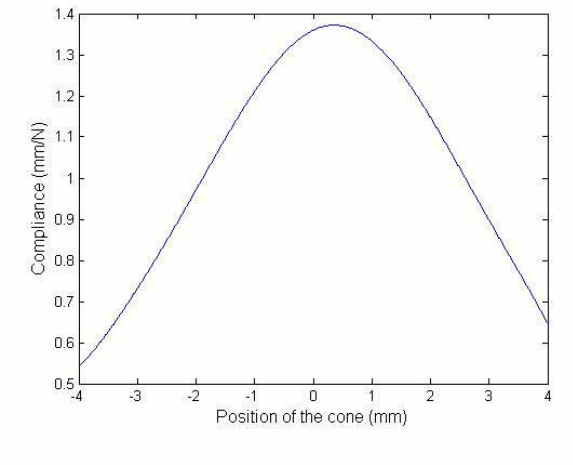

Figure 3: Compliance curve for a typical driver

The nonlinear spring force is given by:

$$F_{sp} = K(x) \cdot x \qquad (3)$$

where $K(x)$ is the nonlinear spring stiffness. Similar to the BL factor, the spring stiffness can be represented by a polynomial,

$$K(x) = \sum_{i=0}^{n} k_i x^i = \sum_{i=0}^{n} \frac{1}{c_i x^i} \qquad (4)$$

where $\sum_{i=0}^{n} c_i x^i$ defines the driver compliance. Figure 2 and 3 show the BL and compliance curve used in the model, respectively. These figures show that as the cone moves away from its equilibrium position the BL factor decreases and the stiffness increases. The process of determining the nonlinear stiffness and BL factor of a given driver is not discussed here; a detailed discussion of this subject is available in the literature [1,2,3]. With these definitions, the differential equation for the mechanical subsystem is given by:

$$M\ddot{x} + B\dot{x} + K(x)x = F = BL(x) \cdot i \qquad (5)$$

where M is the mass of the moving part and B is the mechanical damping of the system.

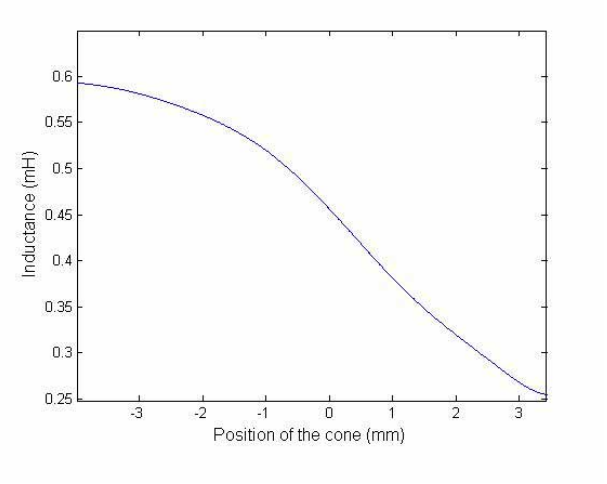

Figure 4: Inductance curve for a typical driver

The electrical subsystem includes the nonlinear inductance and the electrical resistance of the coil. Also included in this subsystem is the model of the existing

back EMF as the coil moves relative to the magnet. The inductance is shown in Figure 4 and is modeled as:

$$Le(x) = \sum_{i=0}^{n} l_i x^i \qquad (6)$$

The differential equation for the electrical subsystem with a voltage amplifier is then given by:

$$Le(x) \cdot \frac{di}{dt} + \mathrm{Re} \cdot i + BL(x) \cdot \dot{x} = V_{in} \qquad (7)$$

where Re is the coil resistance, $BL(x) \cdot \dot{x}$ is the BEMF, i is the current in the coil, and V_{in} is the input voltage to the coil.

In the case of an ideal current amplifier the above equation becomes:

$$G \cdot i = V_{in} \qquad (8)$$

with G a constant, thus eliminating the effect of BEMF and inductance. This in turn will remove the distortion due to nonlinearities in inductance and BEMF [4]. The elimination of the nonlinear BEMF and the subsequent reduction in distortion may however be at the cost of increasing the likelihood of the onset of the jump resonance behavior. To eliminate this adverse side effect, it is necessary to introduce linear damping back into the system.

3. FORCED OSCILLATION

In this section we develop some of the analytical results that explain in more detail the jump resonance phenomenon. To develop an analytical model for this nonlinear behavior a simplified mass, spring, and damper system is considered. The spring is assumed to be nonlinear and of the form:

$$k(x) = k_0 \pm k_1 x^2 \qquad (9)$$

which may describe both stiffening and softening nonlinear spring effect. The undamped forced response is first considered followed by the damped forced response.

3.1. Undamped forced oscillation

To illustrate the jump resonance behavior of a driver, the forced response of the undamped mechanical subsystem is investigated. Given that the mechanical stiffness in a given driver is parabolic (see Figure 3), for simplicity we may write the equation of motion as:

$$M\ddot{x} + [k_0 + k_1 x^2] \cdot x = F \qquad (10)$$

Dividing through by the mass, we get:

$$\ddot{x} + \omega_n + \beta x^3 = P = F / M \qquad (11)$$

where $\beta = k_1 / M$

Assuming a harmonic excitation of frequency ω, and magnitude $P \cdot M$, the equation of motion becomes:

$$\ddot{x} = -\omega_n - \beta x^3 + P \sin(\omega \cdot t) \qquad (12)$$

Let us assume $C \sin(\omega \cdot t)$ to be the first approximation to the solution of the equation of motion, with C a constant. Substituting this assumed solution into our differential equation, we get:

$$\ddot{x}_p = (P - \omega_n^2 C - \frac{3}{4}\beta C^3)\sin(\omega \cdot t) + \frac{\beta C^3}{4}\sin(3\omega \cdot t) \qquad (13)$$

where $\ddot{x}_p$ is the calculated acceleration based on the assumed solution. Integrating this equation twice, and assuming periodicity for x_p, we get a second approximation for the solution of our differential equation, given by:

$$x_p = \frac{C}{\omega^2}(\omega_n^2 + \frac{3}{4}\beta C^2 - \frac{P}{C})\sin(\omega \cdot t) - \frac{\beta C^3}{36\omega^2}\sin(3\omega \cdot t) \qquad (14)$$

Although the first iteration, given by equation 14, provides a satisfactory approximation to the solution of

equation 12, the above procedure may be repeated in order to arrive at a better approximate solution. We shall stop at the present iteration and use the Duffing method to determine the constant in the above approximate solution. Based on Duffing's approach [7-10], the component of the response with frequency equal to ω is set equal in the first and the second approximation, giving:

$$C = \frac{1}{\omega^2}(\omega_n^2 + \frac{3}{4}\beta C^2 - \frac{P}{C}) \cdot C \qquad (15)$$

or

$$\frac{\omega^2}{\omega_n^2} = 1 - \frac{P}{C\omega_n^2} + \frac{3}{4}\frac{\beta}{\omega_n^2}C^2 \qquad (16)$$

Given the mass, nonlinear stiffness, and the forcing function, the above equation can be solved to determine the amplitude of the forced vibration as a function of the excitation frequency, ω. As an example consider the following case:

$$M = 3\times10^{-3}\,kg$$

$$k_0 = 735.6\,N/m$$

$$k_1 = 3.66\times10^{7}\,N/m^3$$

$$|F| = 1.27N$$

Then equation 16 becomes:

$$9.15\times10^{9}C^3 + (2.45\times10^{5} - \omega^2)C - 423 = 0 \qquad (17)$$

and can be solves to find the constant C as a function of the excitation frequency. Keeping the real roots of equation 17 and plotting them versus the excitation frequency result in Figure 5.

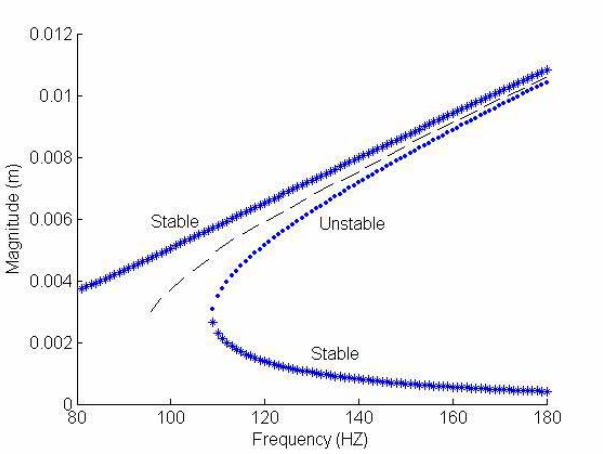

Figure 5: Force response for a nonlinear spring

This figure shows that the frequency response of the nonlinear system is quite different from that of a linear system. In the nonlinear case as many as three different amplitudes of response are possible for a given excitation frequency. Furthermore, the amplitude of response, unlike the linear case, remains finite for all frequencies. It can be seen from Figure 5 that the frequency response curve near the resonance frequency tilts to the right. This tilt is due to the stiffening of the spring at large displacement. It should be noted that, in Figure 5, the points indicated by dots are unstable points and those marked by asterisks are stable points.

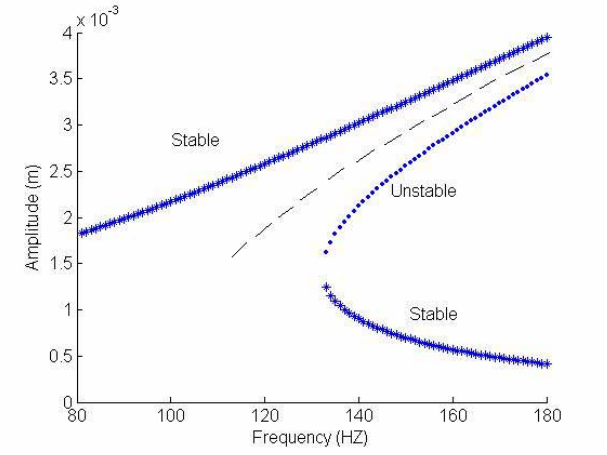

Figure 6: Force response, rapidly stiffening spring

Figure 6 shows the effect of having a spring that stiffens more rapidly as displacement increase. To generate this figure the nonlinear part of the spring was increased to

$k_1 = 2.93\times10^8\, N/m^3$. This higher value of k_1 results in more tilting of the curve and a wider gap.

The results shown in Figures 5 and 6 are valid for a spring that stiffens as displacement increases. In the case of a softening spring the amplitude curve versus excitation frequency is given in Figure 7. Specifically, the curve in Figure 7 corresponds to the case where:

$k_0 = 2035 N/m$, and $k_1 = -3.66\times10^7\, N/m^3$

Unlike the previous figures, this figure shows a curve that is tilting to the left. This tilting to the left, toward the region where the frequency is lower, is in accord with the fact that as the amplitude of motion increases, due to the softening characteristics of the spring, the effective resonance frequency of the system decreases.

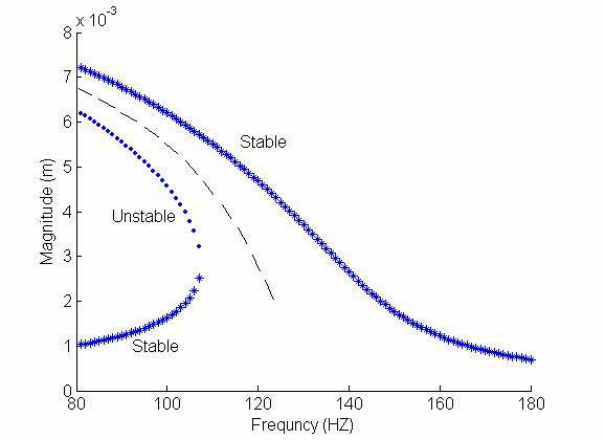

Figure 7: Forced response with a softening spring

3.2. Damped forced oscillation

To this point we have ignored the effect of damping on the nonlinear frequency response of the system. In the interest of brevity, the effect of introducing linear damping is discussed without presenting detailed derivations. In the presence of linear damping a term in $\dot{x}$ will have to be added to equation 10, resulting in equation 18.

$$M\ddot{x} + b\dot{x} + [k_0 + k_1 x^2]\cdot x = F \qquad (18)$$

where b is the damping constant. The magnitude of forced response at a given frequency is then given by:

$$\frac{9}{16}\beta^2 C^6 + \frac{3}{2}(\omega_n^2 - \omega^2)\beta C^4 + \left[(\omega_n^2 - \omega^2)^2 + 4\eta^2\omega^2\right]C^2 = P^2 \qquad (19)$$

where $\eta = \dfrac{b}{2M}$

With $b = 0.32 N.Sec/m$, and the other parameters remaining the same, equation 19 is used to solve for C as a function of the input frequency ω. Plotting the real roots of equation 19 results in Figure 8 showing the amplitude of the response, $|C|$, versus the input frequency for the damped system.

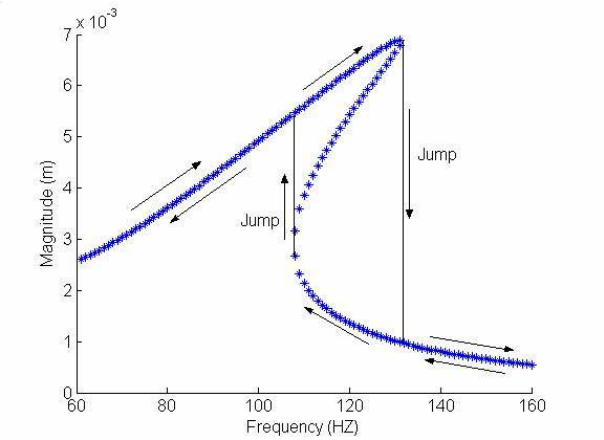

Figure 8: Jump resonance in the presence of damping

Figure 8 shows that unlike the undamped nonlinear response, the stable and unstable parts of the damped response curve merge. It can also be seen from this figure that as the input frequency increases there is a sudden drop in the amplitude of response, and conversely there is a sudden jump in the response amplitude as the input frequency decreases. As indicated by Figure 8, the frequencies at which these sudden jumps in the response amplitude occur are distinct, and dependent on the direction in which the excitation frequency is changed.

A further characteristic of the jump resonance phenomenon is its strong dependence on the level of damping present in the system. Figure 9, shows the change in the response magnitude versus input frequency with decreasing damping. As the figure indicates the jump resonance becomes less and less pronounced as the system damping increases. In fact, at sufficiently high level of damping there is only a minor tilt to the magnitude curve, and no jump behavior can be detected.

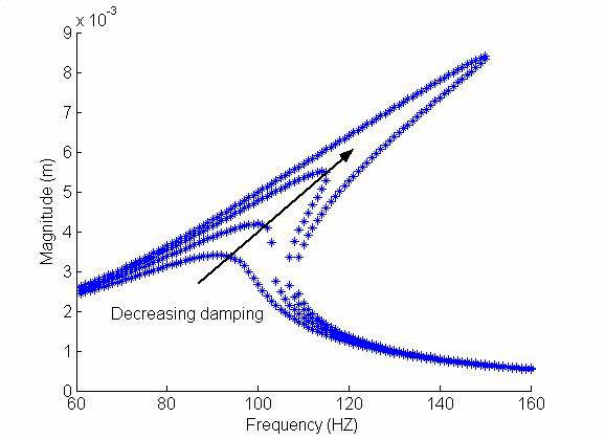

Figure 9: Effect of damping on jump resonance

4. SIMULATION RESULTS

In order to investigate the nonlinear behavior of a typical driver a model of a three inch Vifa driver was created in Matlab and Simulink. The model is based on the equations that were defined in Section 2. The model allows for the driver to be driven with either a voltage or a current amplifier. It includes the nonlinearities in BL factor, spring stiffness, and the inductance.

As discussed in the previous section, in order to observe the jump resonance phenomenon the level of damping in the system has to be low. Given that a current amplifier eliminates the damping effects of BEMF, resulting in a lightly damped system, in order to simulate the jump behavior, the simulations were performed in the current amplifier mode. The response of the driver was simulated in two directions. First, the driver was excited by a chirp signal starting at a frequency of 100 Hz and stopping at 140 Hz over a 40 second total time interval. In the reverse direction, the driver was excited by a chirp signal going from 140 Hz to 100 Hz over a 40 second time interval. The system response was sampled at 10 KHz and stored in a data structure for later analysis. Figure 10 is the simulated envelope of the position response of the driver versus time as the input frequency increases. This figure shows a sudden drop in the amplitude of cone excursion 18 seconds into the simulation. This corresponds to the excitation frequency of: $\omega = 100 + 18 = 118Hz$

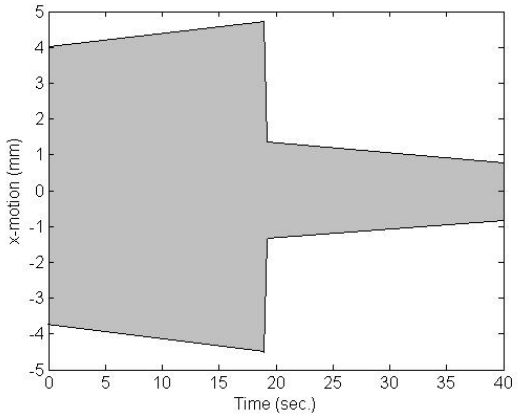

Figure 10: Simulated cone excursion with increasing frequency of excitation

Conversely, Figure 11 is the simulated envelope of the position response of the driver versus time with decreasing input frequency.

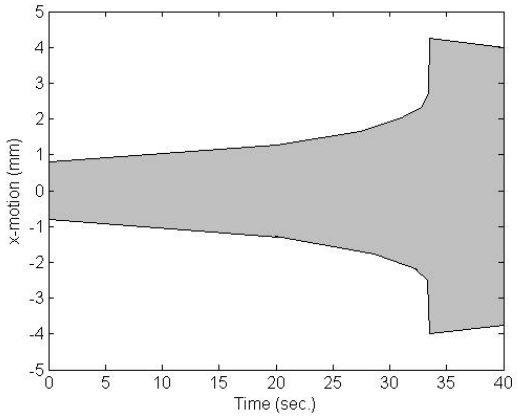

Figure 11: Simulated cone excursion with decreasing frequency of excitation

Figure 11 shows a sudden jump in the excursion amplitude of the cone 34 seconds in to the simulation. This corresponds to the excitation frequency of:

$$\omega = 140 - 34 = 106Hz$$

Figure 12 shows the amplitude of the driver cone displacement versus excitation frequency for both increasing and decreasing input frequency. The forward arrows represent the increasing frequency direction, and the backward arrows represent the decreasing frequency direction.

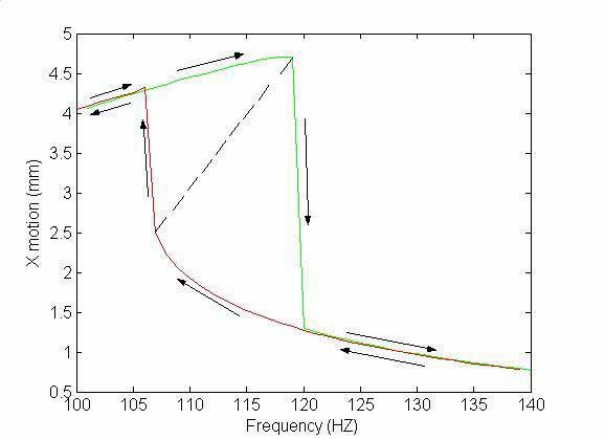

Figure 12: Simulated frequency response with nonlinear BL factor

Figure 12 clearly shows the same behavior that was described in the previous section, and depicted in Figure 8. There is a sudden drop in the response amplitude as the excitation frequency increases, at approximately 118 Hz. Conversely, there is a sudden jump in the response amplitude as the excitation frequency decreases, at approximately 107 Hz.

The model was also used to investigate the effect of other system nonlinearities on the driver jump resonance behavior. Although the jump resonance occurs solely due to the nonlinearities in the stiffness of the driver's surround and spider, the nonlinearities in the BL factor affect the shape of the frequency response curve as well as the specific values of the jump frequencies. In general, for a stiffening spring, greater excitation magnitude causes the jump frequencies to be shifted up in frequency, and widens the gap between the two jump frequencies. Conversely, smaller excitation magnitude causes the jump frequencies to be shifted down in frequency, and reduces the gap between the two jump frequencies. Given that the nonlinear BL factor, as shown in Figure 2, decreases in magnitude as the cone excursion increases, it results in lowering the jump frequencies and narrowing the gap between the two jumps. Figure 13 shows the simulation results with a linear BL factor: note the higher jump frequencies at approximately 109 HZ and 127 Hz, and a wider gap between the two jump frequencies.

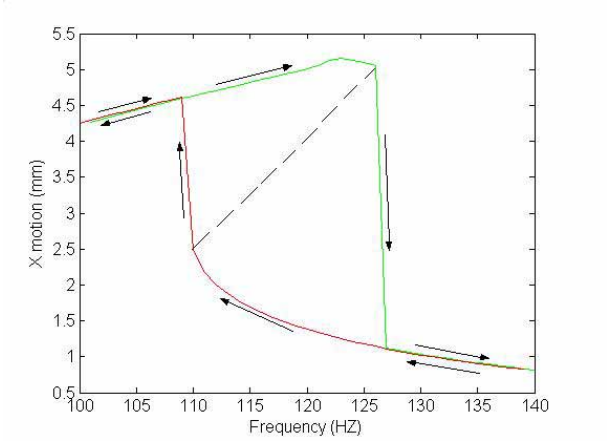

Figure 13: Simulated frequency response with linear BL factor

As shown in this section, the model predicts the nonlinear behavior of a given driver and is in agreement with the analytical results of Section 3. It can be used to conduct parametric studies relating various system parameters to the response of the driver.

5. EXPERIMENTAL RESULTS

A Vifa TC08WD49-08 driver was used to experimentally reproduce the jump resonance phenomenon described in the previous sections. A chirp signal was used to excite the driver with either increasing or decreasing frequency. A current amplifier was used to drive the Vifa transducer, thus eliminating the effect of BEMF damping. The displacement of the cone was measured with a laser displacement sensor and sampled at 10 KHz. The resulting data is analyzed and presented in this section.

Figure 14 is the envelope of the time response of the cone displacement when the driver is excited by a chirp signal, starting at a frequency of 100 Hz and stopping at 140 Hz, over a 40 second total time interval. As shown in this figure, there is an abrupt drop in the amplitude of the cone displacement at approximately 27 seconds into the experiment. This corresponds to the excitation frequency of $\omega = 100 + 27 = 127Hz$.

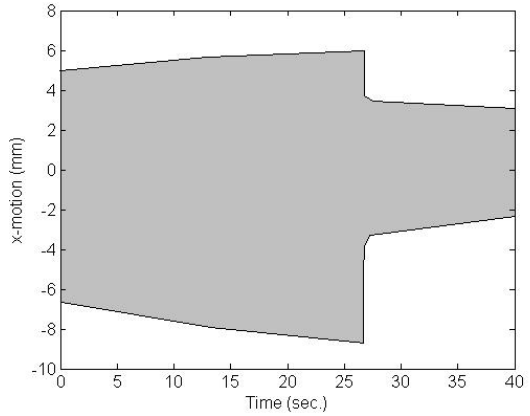

Figure 14: Cone excursion with increasing frequency of excitation.

Figure 15 is the envelope of the time response of the cone displacement in the reverse direction, when the driver is excited by a chirp signal going from 140 Hz to 100 Hz over a 40 second time interval. Again, a sudden jump in the response amplitude is clearly detectable.

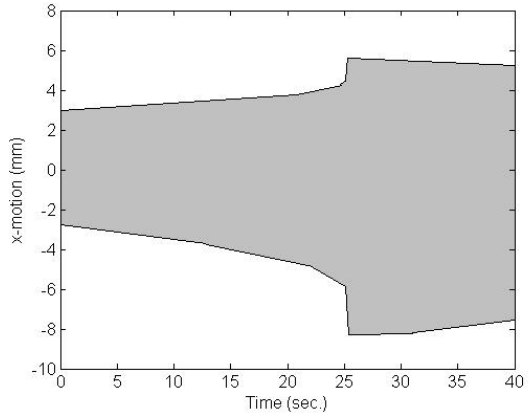

Figure 15: Cone excursion with decreasing frequency of excitation

As shown in Figure 15, there is an abrupt jump in the amplitude of the cone displacement at approximately 25 seconds in to the experiment. This corresponds to the excitation frequency of $\omega = 140 + 25 = 115Hz$.

The amplitude of cone excursion versus the forcing frequency is determined, based on the experimental data, and given in Figure 16. With increasing frequency, an abrupt reduction in the amplitude of excursion occurs at about 127 Hz. Conversely, with decreasing frequency, a sudden jump in the amplitude of cone excursion occurs at about 115 Hz. It should be noted that the low frequency deviation of the two frequency response curves can be attributed to creep and hysteresis in the surround and the spider [11].

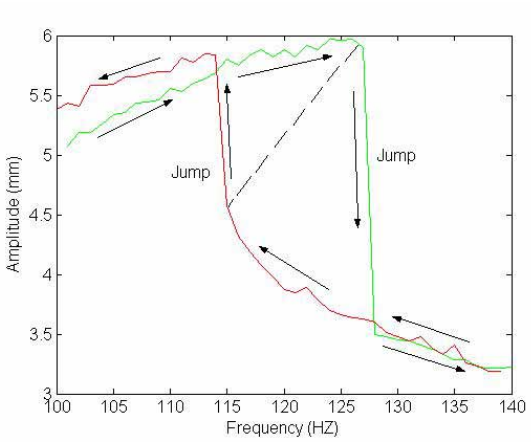

Figure 16: experimental frequency response of a Vifa driver

The experimental results presented in this section show the same jump phenomenon that was described in the previous section. Acoustically, these jumps translate to sudden and very noticeable changes in the acoustic output of the driver.

The differences in the actual jump frequencies between the experimental and the simulated results can be attributed to the mismatch between the model parameters and the actual driver parameters, as well as imperfect match between the drive amplitude in the simulation as compared to the drive amplitude in the experimentation. Other contributing factors are the unmodeled nonlinearities such as creep and hysteresis in the restoring spring, as well as hysteresis in the BL factor.

6. CONCLUDING REMARKS

Most audio transducers have surrounds and spiders that act as nonlinear spring. The nonlinear restoring force that acts on the driver cone can lead to a jump phenomenon, especially under low damping conditions. For instance, if a current amplifier is used to remove the nonlinearities due to BEMF and coil inductance, the resulting loss of damping may lead to the appearance of the jump behavior. This implies that it would be prudent to introduce linear damping to the system to prevent the occurrence of this undesirable jump resonance phenomenon.

7. REFERENCES

[1] Knudsen J., "loudspeaker Modeling and Parameter Estimation," Preprint 4285; 100th Convention; April 1996

[2] Klippel W., "Dynamic Measurement and Interpretation of the Nonlinear Parameters of Electrodynamic Loudspeakers," JAES Vol. 38, No. 12, Dec. 1990

[3] Klippel W., "Measurement of the Large Signal Parameters of an Electrodynamic Transducer," Preprint 5008; Convention 107; August 1999

[4] Mills, P.G.L., Hawksford, M.O.J., "Distortion Reduction in Moving-Coil Loudspeaker System Using Current-Drive Technology," JAES, Vol 37, NO. 3, February 1989

[5] Hanselman D., "Mastering Matlab," (Prentice Hall, 2001)

[6] Harman T., "Mastering Simulink," (Prentice Hall, 2001)

[7] Guckenheimer J., Holmes P., "Nonlinear Oscillations, Dynamical Systems, and Bifurcations of Vector Fields," (Springer-Verlog, 1986)

[8] Verhulst F., "Nonlinear Differential Equations and Dynamical Systems," (Spinger-Verlog, 1989)

[9] Drazin P.G., "Nonlinear Systems," (Cambridge University Press, 1993)

[10] Rand R., "Lecture Notes on Nonlinear Vibrations," Dept. of Theoretical and Applied Mechanics, Cornell University, Ithaca, NY 14853

[11] Knudsen M. H., Jensen J., "Low-Frequency Loudspeaker Models That Include Suspension Creep," JAES vol. 41, No. ½, December 1992

APPENDIX

The polynomial coefficients of the BL factor, spring and inductance used in the simulation, are given by:

$b_0 = 3.5801$ N/A	$b_1 = 0.17891$ N/Amm
$b_2 = -0.1305$ N/Amm^2	$b_3 = -0.004935$ N/Amm^3
$b_4 = -9.609e\text{-}5$ N/Amm^4	$b_5 = -0.000292$ N/Amm^5
$b_6 = -0.0001355$ N/Amm^6	$b_7 = 1.4618e\text{-}5$ N/Amm^7
$b_8 = -2.864e\text{-}6$ N/Amm^8	

Table 1 Polynomial coefficients for BL factor

$c_0 = 1.3594$ mm/N	$c_1 = 0.068382$ 1/N
$c_2 = -0.09151$ 1/Nmm	$c_3 = -0.0078709$ 1/Nmm^2
$c_4 = 0.0047939$ 1/Nmm^3	$c_5 = 0.00049244$ 1/Nmm^3
$c_6 = -0.00017717$ 1/Nmm^4	$c_7 = -1.3531e\text{-}5$ 1/Nmm^5
$c_8 = 3.0196e\text{-}6$ 1/Nmm^6	

Table 2 Polynomial coefficients for compliance

$l_0 = 0.45636$ mH	$l_1 = -0.0739$ mH/mm
$l_2 = -0.00662$ mH/mm^2	$l_3 = 0.005275$ mH/mm^3
$l_4 = 0.000883$ mH/mm^4	$l_5 = -0.000485$ mH/mm^5
$l_6 = -9.537e\text{-}5$ mH/mm^6	$l_7 = 1.875e\text{-}5$ mH/mm^7
$l_8 = 3.9688e\text{-}6$ mH/mm^8	

Table 3 Polynomial coefficients for inductance

R_e =coil resistance =5.5 Ohm
M=Effective mass=3g
b=Linear damping=0.32N.sec/m